

# Metastability of gold-carbonyl cluster complexes, $\text{Au}_N(\text{CO})_M^-$

W.T. Wallace<sup>1</sup> and R.L. Whetten<sup>1,2,a</sup><sup>1</sup> School of Chemistry and Biochemistry, Georgia Institute of Technology Atlanta, GA 30332-0400, USA<sup>2</sup> School of Physics Georgia Institute of Technology, Atlanta, GA 30332-0430, USA

Received 17 April 2001

**Abstract.** Smaller gold-cluster anions, typified by  $\text{Au}_7^-$ , adsorb multiple CO molecules in a high-pressure, room-temperature flow-reactor, tending toward previously unknown saturation compositions,  $\text{Au}_7(\text{CO})_4^-$ . The weakness of the gold-carbonyl adsorption bond is evidenced indirectly by the high CO partial pressure required and more directly by the high probability of fragmentation in the field-free flight region of the reflectron-type time-of-flight mass spectrometer. The analysis of this metastability reveals that the actual distribution  $f_{N,M}$  of products  $\text{Au}_7(\text{CO})_M^-$  in the reactor may be highly non-statistical, *e.g.* with only even- $M$  species present.

**PACS.** 61.46.+w Nanoscale materials: clusters, nanoparticles, nanotubes, and nanocrystals – 36.40.Jn Reactivity of clusters – 36.40.Wa Charged clusters – 82.33.Hk Reactions on clusters

## 1 Introduction

In contrast to the wide range of stable transition-metal carbonyl clusters that have been synthesized (or isolated) and characterized, gold-carbonyl cluster compounds are not known. The probable reasons for this are their high reactivity (supported gold clusters efficiently catalyze CO combustion even at low temperatures [1]) and their very weak binding energy (the  $5d^{10}$  shell is completely filled and lies too deep for effective “promotion”). Only recently have they been detected in the gas-phase, first at low-pressure [2,3] and then in our recent high-pressure flow-reactor investigation [4]. Their main attraction at present is that such complexes may serve as models for the intermediates in the CO reactions catalyzed by supported, small gold particles [1,5,6]. The role of the support is complex and may not be completely understood, but it is believed to involve donation of electron density to the gold [5], hence the emphasis on the cluster anions. Here we report on the CO partial-pressure dependence of the adsorption processes, leading to saturation, and on the identification of additional features in the mass-spectrometrically detected product abundances, corresponding to metastable decay processes that are not observed for stronger binding adsorbates ( $\text{O}_2$ ,  $\text{NO}_2$ ) under the same experimental conditions [7,8]. The unusual (highly nonstatistical) distribution demonstrates that the adsorption, although weak, is not simple, in contrast to the situation with other metals.

## 2 Experiment

The study of metal clusters and their complexes has increased dramatically over the past two decades, due in large part to improvements in time-of-flight (ToF) mass spectrometers [9,10] and the development of laser vaporization techniques for cluster production [11]. A recent review article has summarized much of the progress in the area of metal-cluster reactions [12]. One of the most beneficial improvements to the ToF mass spectrometer has been the addition of a reflectron assembly [10]. This device improves resolution by allowing the total time-of-flight of the ions to be roughly independent of their initial kinetic energy spread. It also facilitates identification of metastable species arising from processes such as collision-induced dissociation or unimolecular decay. Fragmenting ions lose a portion of their mass (corresponding to the neutral fragment) in the first free-flight region, and therefore penetrate the reflecting-field region less deeply and thereby arrive at the detector earlier than their “parent” ions. Reducing the reflection voltage to a critical value causes the parent ions to be transmitted entirely, so that the metastables can be more easily identified. This technique has been used to study ammonia [13] and benzene [14] clusters, as well as other systems of general interest.

A partial schematic of the reflectron ToFMS is shown in Figure 1(a). Gold cluster anions,  $\text{Au}_N^-$ , were produced using a pulsed-helium laser ablation source (a) based on ablating a gold target by the third harmonic of a Nd:YAG laser (355 nm), as described previously [7,4,15]. Cluster growth and primary cooling takes place within the confined flowstream of He buffer gas and secondary cooling occurs upon expansion into vacuum. The cluster beam is

---

<sup>a</sup> e-mail: whetten@chemistry.gatech.edu

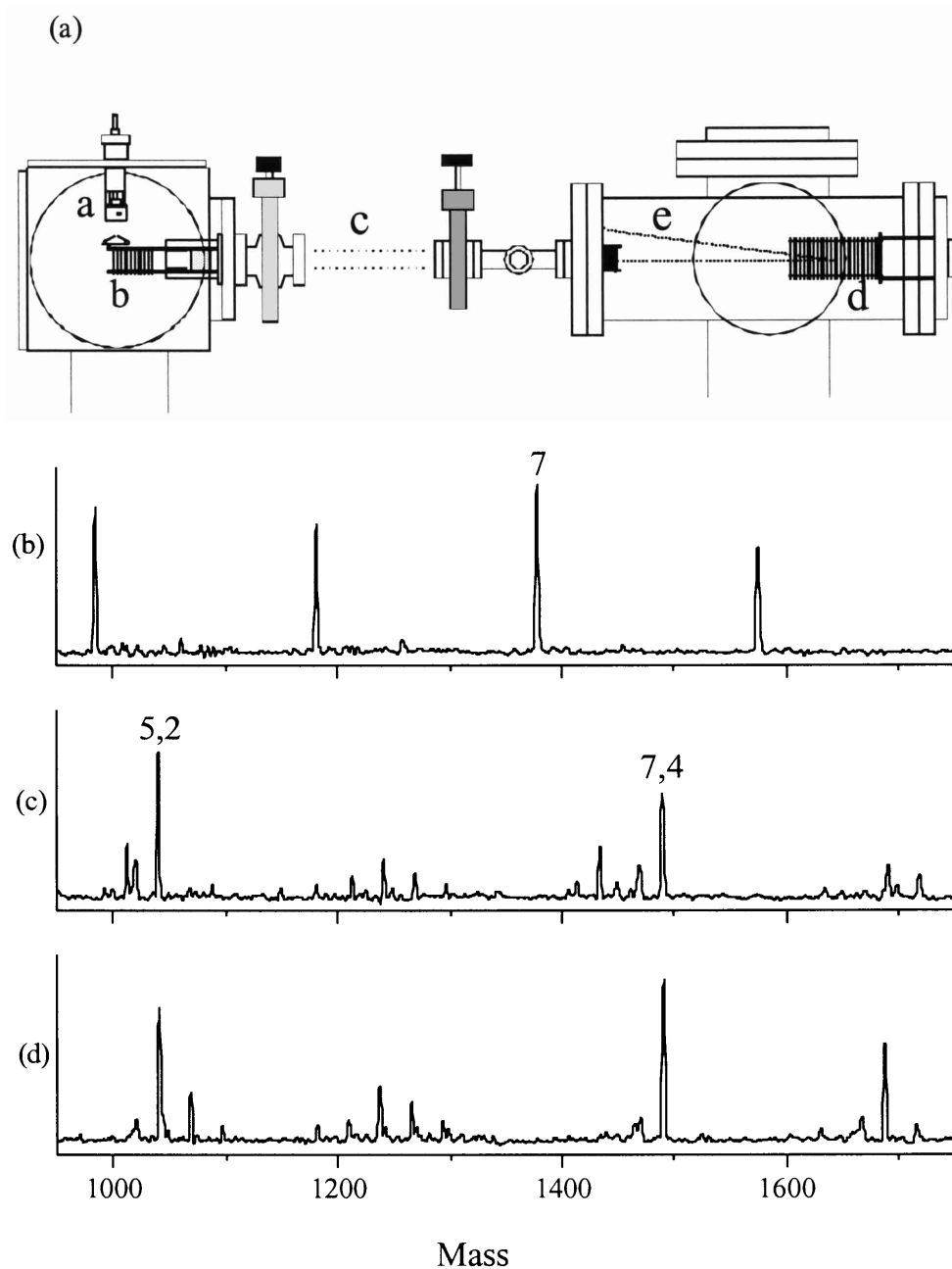


**Fig. 1.** Pulsed flow-reactor experiment with time-of-flight mass-spectrometry detection (a). Schematic illustration of the experimental apparatus, wherein the labels (a through e) indicate the regions mentioned in the text: (a) the cluster-source and isothermal flow-reactor region (field-free), wherein charged clusters and their complexes are generated, respectively. (b) The ion-extraction region of the reflectron ToFMS, which generates the pulsed extraction field. (c) The first field-free flight region. (d) The two-stage reflecting-field region; on entering this region, an ion abruptly loses almost half its kinetic energy in a short, high-field stage, and then penetrates deeply into the long, low-field stage, before turning around; (e) the second field-free flight region, ending at the anion detector (a dual-microchannel-plate assembly). (b) A typical time-of-flight mass spectrum of gold cluster anions ( $\text{Au}_5^-$  through  $\text{Au}_8^-$ ), without CO adsorption complexes; the CO:He gas (from the secondary pulsed gas-valve) has been temporally displaced. The time-scale has been converted to a mass-scale, in amu units, calibrated by reference to a standard  $\text{Cs}_N\text{I}_{N+1}^-$  mass spectrum. (c) as in (b), but with sufficient CO introduced to lead to formation of  $\text{Au}_N(\text{CO})_M^-$  complexes, denoted by  $(N, M)$ . (The two valve pulses are temporally overlapped, and the secondary gas-pulse is a 70% CO:He mixture.) The expected peaks are centered at the masses given by  $197N + 28M$  amu; additional peaks cannot be assigned by this, or any other reasonable, mass combinations. (d) as in (a), but now the CO is introduced upstream, in the primary-valve gas, in a 2% CO:He mixture. Under these conditions, the  $\text{Au}_7^-$  cluster is almost completely converted to a single “saturation” product, namely the  $\text{Au}_7(\text{CO})_4^-$  complex, (7, 4).

skimmed for collimation and the ions are extracted (b) at right angles by the pulsed field of a reflectron-type time-of-flight mass spectrometer. Carbon monoxide was introduced into the flow by two different methods, using various CO:He mixtures. The use of a second pulsed valve to introduce the CO allows reactions to occur after the primary growth and cooling stages. Mixtures of up to 70% CO could be used, with gas pulses of various durations. In the second method, carbon monoxide is introduced into the primary flow by using a CO:He mixture as the buffer gas, causing cluster growth to take place in the presence of both He and CO. Even with as little as 2%, this method allows a much higher partial pressure of CO to be obtained in the reaction zone and may also favor the establishment of equilibrium conditions. For the present experiments, the total extraction voltage (b) of the mass spectrometer was set at 5 kV, while the dual-stage reflectron (d) was initially set at voltages of 2905 V and 2072 V. To achieve the study of the fragmentation patterns of the  $\text{Au}_N(\text{CO})_M^-$  complexes, the secondary voltage of the reflectron (initially 2072 V) was lowered by increments of 5-10 V. With a sufficiently reduced field in the reflection region, those cluster complexes with kinetic energies higher than the reflecting voltage should simply pass through the reflectron and strike the rear of the chamber. However, those complexes of reduced kinetic energy (due to fragmentation from higher mass complexes) should still be reflected toward the detector, e.

### 3 Results and discussion

A clean mass spectrum (no CO added) of gold cluster anions ( $\text{Au}_N^-$ ,  $N = 5-9$ ) can be seen in Figure 1(b). By adding a 70% CO:He mixture through the secondary valve, the spectrum shown in Figure 1(c) is obtained. The addition of the CO leads to depletion of the bare-cluster peak, accompanied by the appearance of the expected peaks associated with the complexes corresponding to  $\text{Au}_N(\text{CO})_M^-$ . By increasing the partial pressure of CO in the reactor, the distribution of product complexes for a given cluster, such as  $\text{Au}_7^-$ , can be shifted from single adsorption toward saturation adsorption. A statistical measure of the extent of adsorption is the mean number of CO molecules adsorbed; this is plotted in Fig. 2 *versus* the duration of the CO:He pulse, a measure of the CO partial pressure in the reactor when the clusters are present. In Fig. 1(d), the saturation adsorption level,  $M = 4$ , of  $\text{Au}_7^-$  has been determined by upstream CO introduction.

However, close inspection reveals a second series of “satellite” peaks, as seen in the expanded figure 3(b). In lieu of these peaks arising from contamination or other processes taking place in the reaction zone of the cluster source, the “extra” peaks could be due to products of metastable decay processes (1) taking place in the first free-flight region (labeled c, in Fig. 1a) of the mass spectrometer:

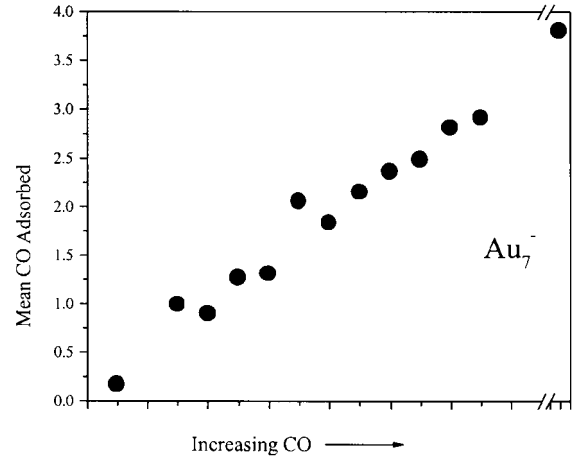
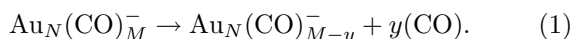


**Fig. 2.** Variable adsorption of CO on  $\text{Au}_7^-$ . By linearly varying the duration of the secondary (CO:He) gas pulse (the horizontal axis), the partial-pressure of CO in the reactor can be adjusted. Consequently, the mean number of CO molecules adsorbed on the  $\text{Au}_7^-$  cluster (the vertical axis) can be varied from null adsorption to nearly three-quarter saturation ( $M = 4$ ) in a single experiment, yielding an adsorption-isotherm type curve. For reference, the mean-adsorption value for upstream CO addition (Fig. 1d) is also plotted, beyond the break in the scale.

For  $y = 1$ , these “satellite” peaks appear approximately 20 amu lower in mass than each  $\text{Au}_N(\text{CO})_M^-$  complex. This idea is relatively simple to test both theoretically and experimentally. Using the same reasoning described previously [13], the difference between the residence times of the parent and daughter ions in the reflectron can be derived. In a simplest calculation, the stopping and turn-around time in the reflectron, given by

$$t = \left( \frac{2mK}{e^2 E^2} \right)^{1/2} \quad (2)$$

where  $K$  is the kinetic energy of the ion,  $m$  is the mass, and  $E$  is the electric field in the turn-around region, will be different for two masses, where  $m' < m$  and  $K' = (m'/m)K$ ,

$$\Delta t = t - t' = \left( \frac{2mK}{e^2 E^2} \right)^{1/2} \left( 1 - \left( \frac{m'}{m} \right)^{1/2} \right). \quad (3)$$

To account for both the entrance into and the exit from the turn-around region,  $2\Delta t$  must be found. In the present settings of the reflectron,  $E = 2072 \text{ V}/8.9 \text{ cm}$  and  $K$  can be approximated to be 2900 eV under the circumstances that the initial kinetic energy of the ions is nearly 5000 eV and the first reflectron stage dissipates 2100 eV. Using the mass of the  $\text{Au}_6(\text{CO})_1^-$  cluster, 1210 amu, and its metastable decay counterpart,  $\text{Au}_6^-$ , 1182 amu, the difference in the time of arrival at the detector for the two species can be found to be  $\sim 523 \text{ ns}$ . The experimental results show a  $\Delta t$  of approximately 400 ns. There is a spread in the peaks of  $\sim 200 \text{ ns}$  (FWHM). If the extra peaks are in fact resulting from metastable decay

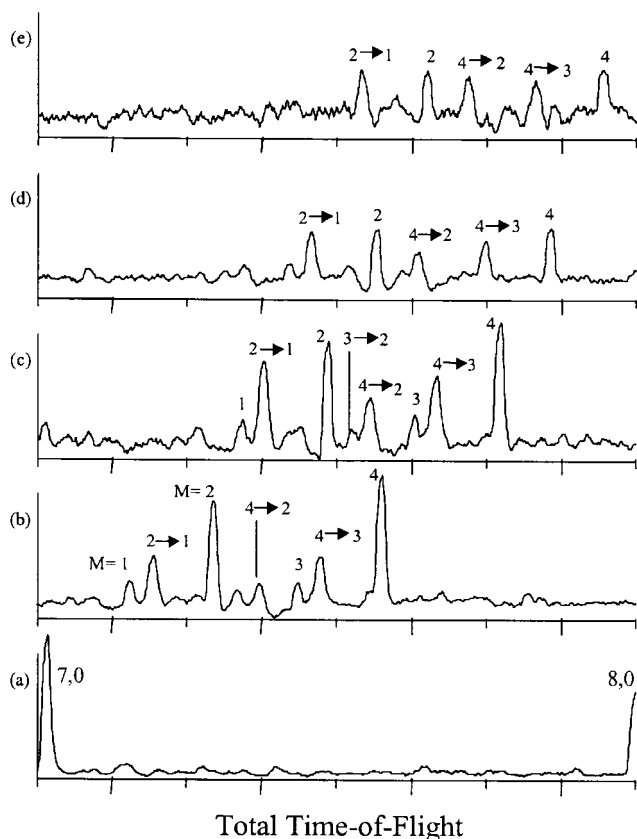


**Fig. 3.** Identification of metastable decay products. Expanded region from a series of time-of-flight mass spectra, showing the effect of reducing the voltage applied to the second stage of the reflecting field region (labeled d in Fig. 1a). In part (a), a mass-spectrum of  $\text{Au}_N^-$  clusters (no CO introduced) is plotted, for reference, cf. Fig. 1b. In part (b), multiple CO adsorption is evident, much as in the case of Fig. 1c. For parts (b) through (e), the cluster source and reactor conditions are held constant, while the total voltage applied to the second-stage of the reflecting field region is 2072 V (b), to 1945 V (c), 1895 V (d), and 1845 V (e). The labels indicate both stable complexes (no arrow) as well as metastable decay products (with an arrow indicating the identified decay process).

processes in the first free-flight region of the mass spectrometer, a decrease in the reflectron voltage should result in the decrease of the parent mass peaks, leaving only the metastable peaks. As can be seen in Figure 3, this relative enhancement of the metastable peaks does indeed occur. The persistence of the extra peaks proves they are due to decay processes, as opposed to contamination or other reactions. Metastable decay may result from the internal energy of the ion as it leaves the source (@300 K), or it may be caused by collisions with background gas in the flight path. In preliminary collision-induced dissociation (CID) measurements, Lee found that the CID threshold energies of CO on small gold clusters,  $N < 7$ , were fairly small [16]. In the case of the initial CO binding on  $\text{Au}_6^-$ ,

the binding energy was  $0.87 \pm 0.13$  eV and the values were even smaller for  $\text{Au}_4^-$  and  $\text{Au}_3^-$ . It is possible that the binding of CO with  $\text{Au}_N^-$  clusters is very weak, and any excess reaction energy causes the reaction complexes to decay. In fact, we have recently found that, in the pressure accessible to us, CO will not bind to  $\text{Au}_2^-$  or  $\text{Au}_3^-$  at room temperature, although these clusters have been shown to bind CO at much lower temperatures [4,17]. In any case, under the same experimental conditions, mass spectra of more strongly binding adsorbates ( $\text{O}_2$ ,  $\text{NO}_2$ ) did not show such features [7,8].

While this study raises several interesting questions concerning the interaction of CO with  $\text{Au}_N^-$ , it corresponds well with much of the previous information provided for the system, and could perhaps aid in the understanding of the reaction mechanisms of CO and  $\text{O}_2$  which occur on supported gold clusters.

The authors would like to thank W.A. de Heer for stimulating discussions concerning this research, B.E. Salisbury for technical assistance, and U. Heiz and L. Wöste for communicating results prior to publication. This work has been supported by the U.S. National Science Foundation.

## References

1. M. Haruta, N. Yamada, T. Kobayashi, S. Iijima, *J. Catal.* **115**, 301 (1989).
2. M.A. Nygren, P.E.M. Siegbahn, C. Jin, T. Guo, R.E. Smalley, *J. Chem. Phys.* **95**, 6181 (1991).
3. T.H. Lee, K.M. Ervin, *J. Phys. Chem.* **98**, 10023 (1994).
4. W.T. Wallace, R.L. Whetten, *J. Phys. Chem. B* **104**, 10964 (2000).
5. A. Sanchez, S. Abbet, U. Heiz, W.D. Schneider, H. Hakkinen, R.N. Barnett, U. Landman, *J. Phys. Chem. A* **103**, 9573 (1999).
6. M. Valden, X. Lai, D.W. Goodman, *Science* **281**, 1647 (1998).
7. B.E. Salisbury, W.T. Wallace, R.L. Whetten, *Chem. Phys.* **262**, 131 (2000).
8. W.T. Wallace, R.L. Whetten, to be published.
9. V.A. Mamyryn, V.I. Karateav, D.V. Schmikk, V.A. Zaugin, *Sov. Phys. JETP* **37**, 45 (1973).
10. H. Kuhlewind, H.J. Neusser, E.W. Schlag, *Int. J. Mass Spectrom. Ion Phys.* **51**, 255 (1983).
11. T.G. Dietz, M.A. Duncan, D.E. Powers, R.E. Smalley, *J. Chem. Phys.* **74**, 6511 (1981).
12. M.B. Knickelbein, *Annu. Rev. Phys. Chem.* **50**, 79 (1999).
13. O. Echt, P.D. Dao, S. Morgan, A.W. Castleman Jr, *J. Chem. Phys.* **82**, 4076 (1985).
14. K.E. Schriver, A.J. Paguia, M.Y. Hahn, E.C. Honea, A.M. Camarena, R.L. Whetten, *J. Phys. Chem.* **91**, 3131 (1987).
15. B.E. Salisbury, Ph.D. thesis, Georgia Institute of Technology, 1999.
16. T.H. Lee, Ph.D. thesis, University of Nevada-Reno, 1995.
17. U. Heiz, L. Wöste, private communication.